

6-22-2020

## A spatial localization of structural degradation areas in the single crystal turbine blades by means of a neutron tomography method

K. M. Nazarov

*L.N. Gumilyov Eurasian National University; Joint Institute for Nuclear Research ,Kazakhstan*

S. E. Kichanov

*Joint Institute for Nuclear Research ,Russian Federation*

E. V. Lukin

*Joint Institute for Nuclear Research ,Russian Federation*

A. V. Rutkauskas

*Joint Institute for Nuclear Research ,Russian Federation*

B. N. Savenko

*Joint Institute for Nuclear Research ,Russian Federation ,*

Follow this and additional works at: <https://www.ephys.kz/journal>



Part of the [Materials Science and Engineering Commons](#), and the [Physics Commons](#)

### Recommended Citation

Nazarov, K. M.; Kichanov, S. E.; Lukin, E. V.; Rutkauskas, A. V.; and Savenko, B. N. (2020) "A spatial localization of structural degradation areas in the single crystal turbine blades by means of a neutron tomography method," *Eurasian Journal of Physics and Functional Materials*: Vol. 4: No. 2, Article 2. DOI: <https://doi.org/10.29317/2020040202>

This Original Study is brought to you for free and open access by Eurasian Journal of Physics and Functional Materials. It has been accepted for inclusion in Eurasian Journal of Physics and Functional Materials by an authorized editor of Eurasian Journal of Physics and Functional Materials.

# A spatial localization of structural degradation areas in the single crystal turbine blades by means of a neutron tomography method

K.M. Nazarov<sup>\*,1,2</sup>, S.E. Kichanov<sup>2</sup>, E.V. Lukin<sup>2</sup>,  
A.V. Rutkauskas<sup>2</sup>, B.N. Savenko<sup>2</sup>

<sup>1</sup>L.N. Gumilyov Eurasian National University, Nur-Sultan, Kazakhstan

<sup>2</sup>Joint Institute for Nuclear Research, Dubna, Russia

e-mail: knazarov@jinr.ru

DOI: 10.29317/2020040202

Received: 10.03.2020 - after revision

The single crystal nickel-based superalloy turbine blades have been studied by means of a neutron tomography method as a non-destructive structural probe. Differences in neutron attenuation coefficients inside volume of metal bodies of the turbine blades have been found. Those observed differences could be associated with inner structural incoherence areas arising in the process of operation of the turbine blades. Applications of special algorithms for a three-dimensional imaging data analysis allow obtaining a spatial distribution of those areas inside the turbine blades and estimate those volumes. To study a temperature evolution of structural incoherence areas, the additional neutron tomography studies of the turbine blades with thermal treatment were performed.

**Keywords:** turbine blades, superalloys, neutron tomography, three-dimensional reconstruction, image processing.

## Introduction

The turbine blades and vanes, combustor elements and rotors made of nickel-aluminum superalloy materials are widely used in aircraft and gas-pumping turbines, rocket engines, in the components for nuclear and chemical processing

plants [1-3]. The distinguished high-temperature strength and toughness, a creep and corrosive resistance are functional properties of those industrial components [3].

The structural dendritic arms form a structure of the Ni-based superalloy single crystals [4, 5]. The orientations of those dendrite arms respect to the applied stress or thermal gradients directions improve the mechanical properties of superalloy single crystals components [4, 6]. In other hands, the unique mechanical and physical properties of nickel-based single crystal materials on a microstructural level are a result of a binary type of structural organizations [2, 7, 8]. Then metal dopants added to initial nickel compound, the so-called  $\gamma'$ -phase embedded in solid-state  $\gamma$ -phase occurs [2, 8]. Those  $\gamma$  and  $\gamma'$ -phases are structurally similar and coherent, but they show different mechanical properties resulting in two different deformation mechanisms. A propagation of the mobile dislocations predominantly formed in the  $\gamma$  matrix prevented by  $\gamma'$ -phase inclusions, leading to the hardening effect in superalloy single crystals [7, 9]. One of unique microstructural properties of  $\gamma'$ -phase is directionally coarsening under high temperature or mechanical stresses during service operation. In this case, cubic particles of  $\gamma'$ -phase transform into the layered plates or a raft structure [2, 9-11]. The rafting is an origin of creeps and cracks in nickel-base superalloy materials and a reason of degradation of the mechanical properties of certain industrial products.

The stringent requirements for mechanical properties of superalloy components provoke the detailed systematic structural studies of Ni-based single crystal materials. The based on the experimental data comprehensive models for a prediction of a structural degradation inside industrial products are essential. The systematic structural studies can provide requested data for non-destructive diagnostic of the fatigue states of single crystal superalloy components [5, 10, 12]. One of the non-destructive methods is X-ray tomography, which allows acquiring a three-dimension (3D) data with good accuracy and precision for use in both qualitative and quantitative studies. Recently, this method was attracted for studies of a structural aspect of the rafting and for visualization of rafting tunnels with nanometer scale inside single crystal superalloy materials [8, 9, 13]. However, X-ray tomography methods, including ones on synchrotron radiation sources, have some limitations related to the high absorption of X-rays in nickel, because of which thickness of investigated samples restricted a few tenths of a millimeter [14]. A complementary method to X-ray tomography is a neutron tomography. This method is the powerful tool of non-destructive analysis, which demonstrates importance in industrial and scientific research [15]. The fundamental difference in a nature of neutrons interaction with matter compared to X-rays provides additional benefits to neutron methods, including sensitivity to light elements, the notable difference in contrast between neighboring elements, the volumetric studies of large metallic objects. Recently, it was reported, that neutron tomography method provides a visualization of structurally distortion areas inside single crystal objects [16]. In relation to the single crystal turbine blades may be noted that the interdendritic gaps, the residual stress and microcracks can provoke a local structural incoherence regions inside the single crystal and, as

a consequence, an increase of the neutron attenuation because of an additional neutron scattering effect [16, 17]. Regarding the single crystal turbine blades, the millimeter-scaled areas of structural degradation inside metal volume are origins of fatigues and cracks formation. In this way, the neutron tomography method can give essential structural data for the non-destructive detection of local areas of structural incoherence inside massive superalloy components [5, 16]. In our work, we demonstrate the capabilities of neutron tomography method for non-destructive testing for spatial localizations of areas of structural degradation or exuding mosaicity inside of whole volumes of industrial single crystal turbine blades, which are used in gas-pump engines.

## Material and experimental method

The single crystal turbine blades are received as they are. We have tested several blades with long operating time up to 18000 h, where the primary structural rafting as structural degradation effect is expected. The photo of one of studied turbine blades is shown in Figure 1a. The top complex bent blade and bottom massive locking support are main parts of the turbine blade. We measured several turbine blades with same operation time, but the obtained neutron data is almost similar to all turbines blades.

The neutron tomography experiments have been performed at neutron radiography and tomography facility [18, 19] placed on the 14th beamline of the high flux pulsed reactor IBR-2. The IBR-2 reactor provides a thermal neutron beam with wavelengths ranged from 0.2 to 8 angstrom and a spectral distribution maximum of 1.8 angstrom. The presented spectral distribution of neutrons allows detecting well a difference between crystalline and perfect single crystal regions due the additional scattering losses [16, 17]. The set of neutron radiography images have been collected by the CCD-based detector system with maximal field-of-view of 17\*17 cm. The tomography experiments have been performed with rotation step of 0.5° and the total number of measured radiography projections was 360. The exposure time for one projection was 10 s and resulting measurements lasted for 4 h. The obtained in experiment imaging data were subtracted by the camera dark current image and were normalized by the image of the incident neutron beam using the ImageJ software [20]. The tomographic reconstruction was performed by H-PITRE software [21]. As result, a large data containing volume distribution of the 3D pixels (voxels) are collected. The size of one voxel in our studies are 87\*87\*87 μm. Each of the voxels is characterized by the spatial coordinates in the reconstructed 3D volume and a beam attenuation coefficient which is related to a certain gray value. The initial 32-bit images of tomography slices were converted in 16-bit ones, where gray-shades scale leads in range 0-65536 r.u. A 3D volume data of voxels is the essence of the spatial distribution of values of the neutron attention coefficients inside of the total volume of the turbine blade. An attenuation of a neutron beam corresponds to scattering and absorption losses inside a matter. It is accepted, that neutron attenuates processes are described by total scattering cross-sections as the sum of neutron scattering and absorption cross-sections or by

an attenuation length [14, 15].

The VGStudio MAX 2.2 software of Volume Graphics (Heidelberg, Germany) was used for the visualization and analysis of reconstructed 3D data. The distinct visualization of volume areas with disordered grains was achieved by special plugin Local Thickness [22] for ImageJ software.

## Results

A typical example of the neutron radiographic image of the turbine blade is shown in Figure 1b. A complex network of inner cooling channels contrasts well with the metal body of studied blades in the neutron radiography experiments. The tomography reconstruction yields a set of 1263 virtual slices with a thickness of 87  $\mu\text{m}$ . The obtained horizontal virtual slices were loaded to VGStudio MAX software for analysis of 3D volume of the turbine blade. A reconstructed 3D model of the studied turbine blade is presented in Figure 2a.

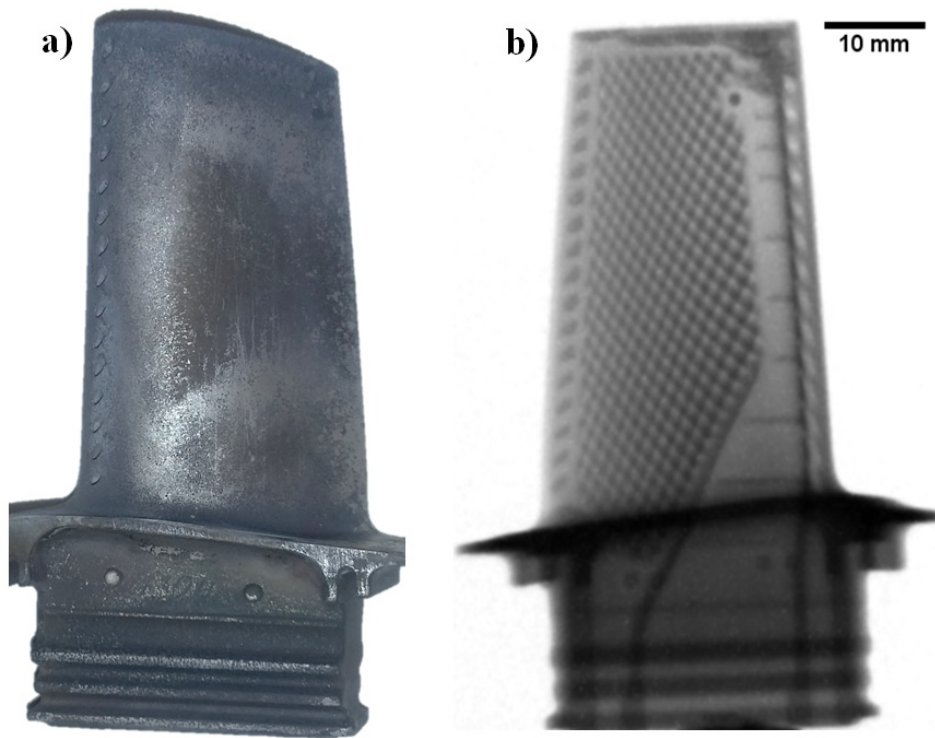


Figure 1. a) The photography of the one of studied turbine blade. A height of the blade is 7 cm. b) The neutron radiography image of the studied turbine blade. The dark regions inside turbine blade correspond to cooling channels in the metal component.

The 3D virtual model of the network of inner cooling channels is well visible. As an example, several images corresponded to different transverse slices of the studied turbine blade are presented in Figure 2b-d. As an unexpected result, a perceptible anisotropy of the attenuation of neutron beam inside Ni-bases alloy body is observed. The tree-dimension areas with high neutron attenuation coefficient locate in top part of the blade, on the facial curved part of the blade and several regions inside locking support (Figure 2b-d). Those areas not respect

to the possible chemical changes on blades surfaces due to contact with air or a cooling fluid and have a pronounced volumetric character (Figure 2b-d). Based on previous results [5, 16], those areas with high neutron attenuation effect can be associated with structural degradation areas inside single crystal turbine blade body.

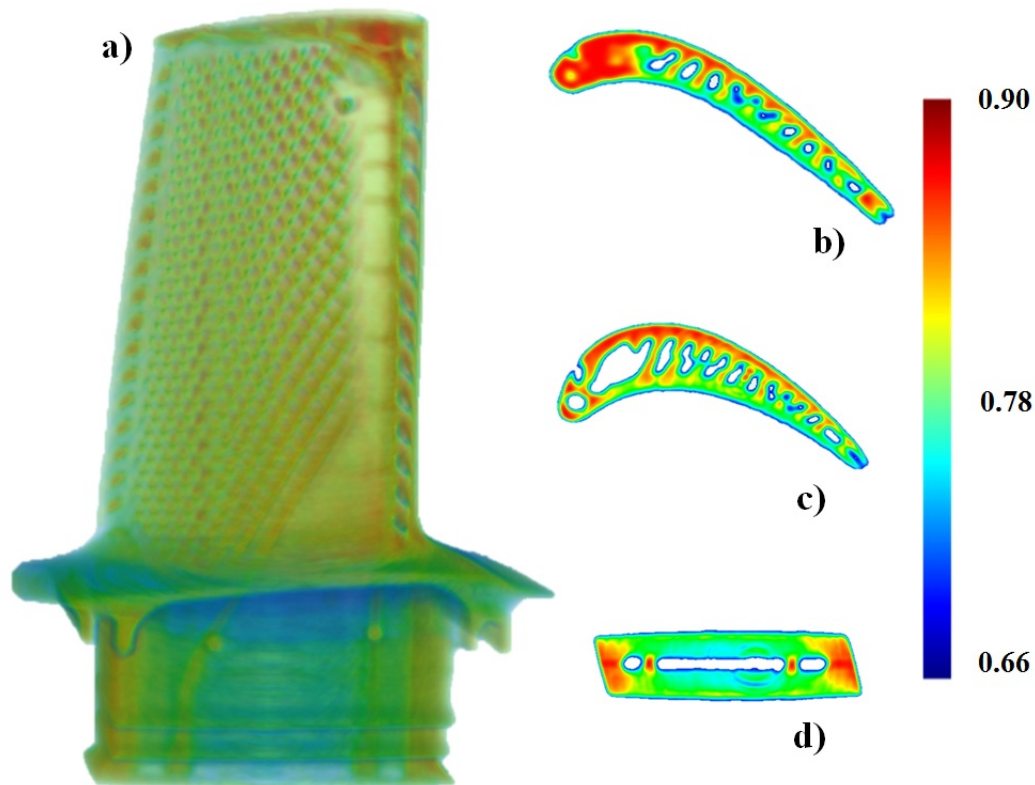


Figure 2. a) The rendered 3D model of the turbine blade with transparency effect after the tomographic reconstruction. b)-d) The examples of the virtual tomography slices of the studied turbine blade which illustrated an anisotropic distribution inside metal body. The slices are corresponded to upper (b) and middle (c) parts of blade component and middle part of the locking support part. A rainbow-like coloring corresponds to a range of neutron attenuation degree from lower (blue) to higher (red). The rainbow-like scale bar of an attenuation coefficients range is shown.

A voxels distribution on neutron attenuation coefficients of an integral histogram of the turbine blade is shown in Figure 3. A range of attenuation coefficients  $<0.66 \text{ cm}^{-1}$  respects to a background. There are three distinguishable peaks on the region of histogram corresponded to neutron attenuations in the turbine blade. We propose the following description of the observed regions on the histogram. The first peak at  $0.85 \text{ cm}^{-1}$  is corresponded to close to the ideal Ni-based single crystal. Due to interactions with air or cooling liquid, the chemical composition on surfaces of turbine blades and inner channels are differing to compare to inner metal volume. It is the reason to adding to total neutron attenuation lengths from thin cover film and the second peak at  $0.79 \text{ cm}^{-1}$  is observed. The peak at  $0.73 \text{ cm}^{-1}$  in the region of low neutron attenuation coefficients corresponds to the structurally degraded areas.

The volumetric calculations based on experimental data have been performed. We had separated the areas with high neutron attenuation coefficients from a total volume of the turbine blade. The volume of those areas forms by 3828296

voxels, what corresponded to volume  $2520.93(2) \text{ mm}^3$ . The total volume of the whole turbine blade is  $41988672$  voxels or  $27649.67(1) \text{ mm}^3$ . Thus, the structural degraded regions estimated occupy up to 9.1% of the total volume of the turbine blade.

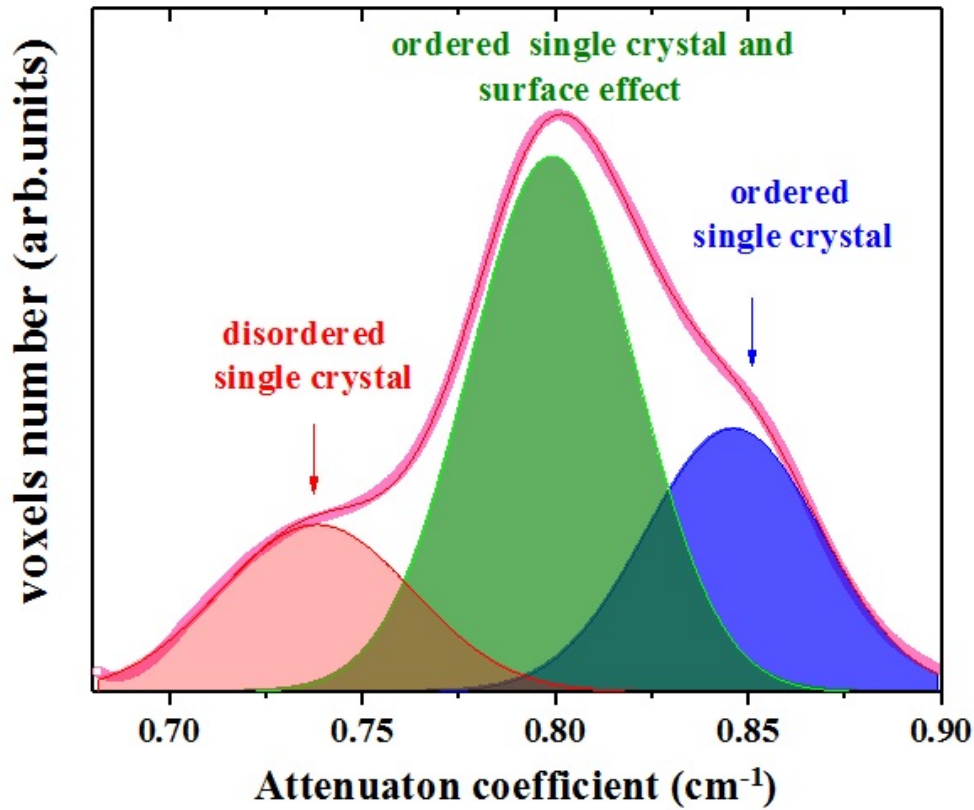


Figure 3. A histogram of the attenuation coefficients of the turbine blade. The peaks corresponded to different regions related to different neutron attenuation coefficients inside turbine blade body are marked.

We applied the special Local Thickness algorithm [22] for the 3D data treatment to improve the visual localization of the structurally degraded regions. A spatial distribution of a density of the neutron attenuation coefficients corrected for a complex 3D shape of investigated turbine blade is the result of those calculations. The obtained 3D model is presented in Figure 4a-c. Clearly, the structural disorder areas are localized in three separate regions of the turbine blade: a roundish region on the upper edge of blade part, a triangular shaped area at the junction of blade and locking support and a lateral one on the locking support. The upper rounded area of the average diameter of 7 mm and volume of  $171.44 \text{ mm}^3$  is connected to a technological plug of the cooling channels inside a turbine blade. The structural disorders in the middle part of the turbine blade are distributed along metal walls between cooling channels. The large volumes of structural disorder areas locate on side parts of locking support (Figure 4a-c) and observed volume of them is  $1236.9 \text{ mm}^3$ .

A simple explanation of the origins of the structural degradation inside turbine blade volume is the presence of residual stresses arising during technical operation of the turbine blade and amplified due to complexities of the shape of the blade.

Recently, the finite elements calculation [23] predicted the large stress around a joining place of the turbine blade, where the blade and locking support are connected. Those stresses are sufficient for the raft structure growth, which in turn causes the structural incoherence inside the single crystal body. In addition, the high temperature and its gradients contribute to an evolution of structural degraded areas [2, 6].

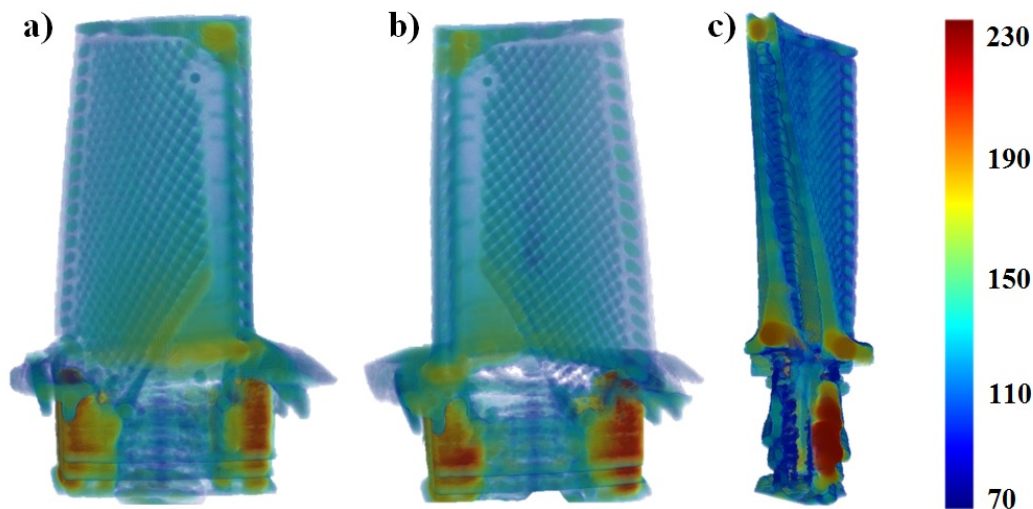


Figure 4. The obtained after calculation by Local Thickness method 3D model of the turbine blade. A coloring schema where a density of neutron attenuation degree extends from low (blue) to high (red) is used. The light transparency effect applied for visibility improvement. a) The facial view of 3D model of the turbine blade. b) Back view of 3D model of the turbine blade. c) A virtual slice of 3D model of the turbine blade, which demonstrates the inner volume of the turbine blade. The corresponded rainbow-like scale bar is shown.

In order to study a temperature evolution of structural degraded regions as well as to discard the possibility of the influence of the methodological factors or image treatments on neutron tomography results, we had performed additional experiments with especially thermally treated turbine blades. One of turbine blade has been annealed at the temperature of  $1050^{\circ}\text{C}$  for 8 h, at which the formation of a raft structure as well as the structural degradation inside single crystal is exactly expected [6, 7, 24]. Another turbine blade was annealed at the temperature of  $600^{\circ}\text{C}$  when mobile dislocations pinned and increases of structural ordering degree are predicted [6, 25].

The 3D model of the spatial distribution of the density of the neutron attenuation lengths inside single crystal body of turbine blade annealed at temperature of  $1050^{\circ}\text{C}$  is presented in Figure 5a. There is an evident increment in the volume of the previously detected structural degraded areas. Thus, the volume of areas on side parts of locking support increases up to  $8879\text{ mm}^3$  or 7 times. The upper rounded area expands to  $243.58\text{ mm}^3$ . The drastic changes in the area located on the jointing between the blade parts and locking support are observed. The structural degradation extend to the platform of locking support at annealing.

The 3D data obtained after applying the Local Thickness method for 3D data of the turbine blade annealed at the temperature of  $600^{\circ}\text{C}$  is shown in Figure 5b. In contradistinction to the previous one, reductions of volumes of structural disorder

areas have been observed. The upper rounded area shrinks to  $110 \text{ mm}^3$ . The volume of structural incoherence areas locates on side parts of locking support decreases down to  $902.76 \text{ mm}^3$ . The area on the jointing between the blade and locking support has not changed noticeably.

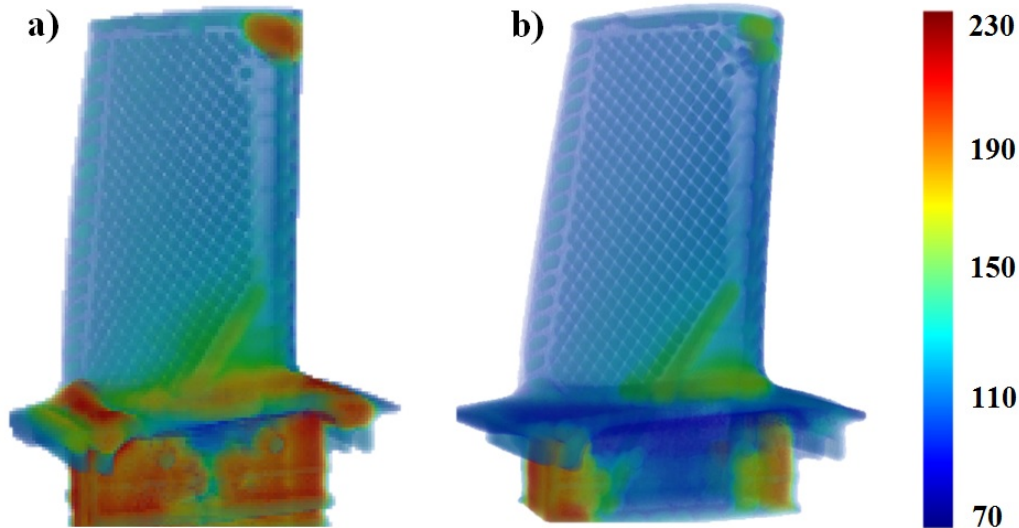


Figure 5. The obtained after calculation by Local Thickness method 3D model of the turbine blades, which are thermally treat. A coloring schema where a density of neutron attenuation lengths degree extends from low (blue) to high (red) is used. The light transparency effect applied for visibility improvement. a) The 3D model of the turbine blade annealed at  $1050 \text{ }^\circ\text{C}$ . b) The 3D model of the turbine blade annealed at  $600 \text{ }^\circ\text{C}$ . The corresponded rainbow-like scale bar is shown.

The smoothing distribution of voxels on the grey-shade scale (histogram) for 3D models obtained by the Local Thickness algorithm and respected to the turbine blades unannealed, annealed at  $600 \text{ }^\circ\text{C}$  and annealed at  $1050 \text{ }^\circ\text{C}$  are shown in Figure 6. We convert obtaining imaging data in 8-bit data for improving the perception of results. Here, the gray-shade scale leads in range 0-256 relative units (r.u.), where 3D volume data of voxels is the distribution of values of the density of neutron attention coefficients or an essence of a degree of structural disordering inside the turbine blades. So, the range of gray-scale  $<35$  r.u. respects to a background component or a fully neutron transparent matter. The set of intensive broad peaks in the histogram from 35 to 140 r.u. corresponds to neutron losses inside the turbine blade bodies. We assumed, that range above 150 r.u. corresponds to neutron attenuations because of structural incoherence areas. Under annealing at temperature  $600 \text{ }^\circ\text{C}$  the triple peak in range 150-180 r.u. on the corresponded histogram decrease, at the same time, an intensity of peaks in the range 180-240 r.u. remains the same. The total number of voxels corresponded to structural incoherence areas decreases. The smoothed histogram of the calculated 3D model of the turbine blade annealed at  $1050 \text{ }^\circ\text{C}$  is characterized by the intense broad peak at 170-250 r.u. It corresponds to the grown of the volumes of the structural degraded areas inside the studied turbine blade under thermal treatment.

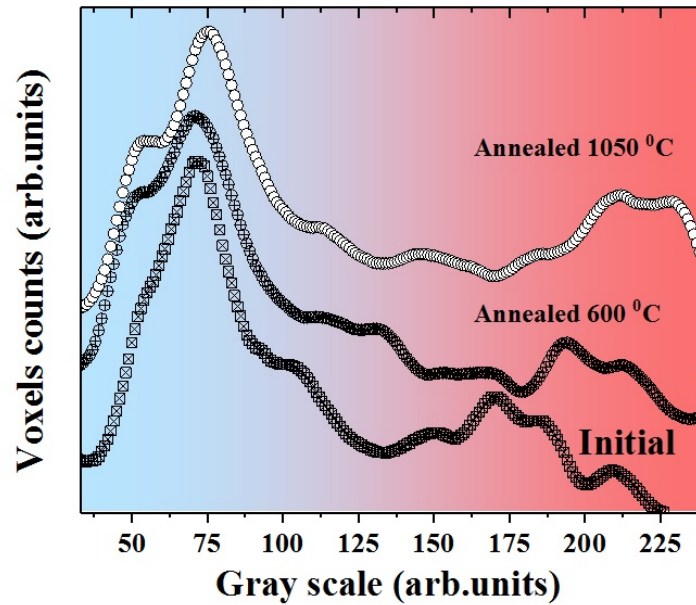


Figure 6. An integral histogram of the gray-shades scale of 3D models of the turbine blade after calculation by the Local Thickness method. The volumetric density of neutron attenuation lengths, as a measure scale for structural disorder degree, extends from more transparent to neutrons a single crystal state (blue region) to structural disorder regions (red color) corresponded to more neutron absorbing areas.

## Conclusion

The obtained visual results have demonstrated the capabilities of neutron tomography method for non-destructive testing for spatial localizations of structural degraded areas inside of the whole volume of the industrial single crystal turbine blades. It is assumed, that the detected structurally incoherence areas are caused by residual stresses arising during the operation of the turbine blades. The application of high-resolution neutron diffraction as a direct method for studying residual stresses is more preferable. However, the requirements for achievable in the experiment gage volume, correct separation of gage volume from complex shaped objects and long scanning times for obtaining a full map of stresses restrict this method as a fast probing technics. In contrast, the optimization of experimental technology for the neutron radiography method, a development of modern fast computation methods for tomography reconstruction and 3D data analysis derive the neutron tomography as a fast non-destructive testing method for the primary localization of structural related dissimilarities, control over their evolution under operation factors, the estimation of crack and fatigues growth. The obtained 3D data can be useful for an optimization of the scan during neutron stress diffractometry, and for developing of modeling theories of the mechanical stability and dislocation and cracks formation inside single crystal turbine blades.

## References

- [1] A. Czyska-Filemonowicz et al., *Inzynieria Materialowa*. **128** (2007) 128.
- [2] T. Pollock et al., *J. Prop. Pow.* **22** (2006) 361.
- [3] J.Chen et al., *Prog. Nat. Sci. Mat.* **20** (2011) 61.
- [4] C.Yang et al., *Prog. Nat. Sci. Mat.* **22** (2012) 407.
- [5] S. Peetermans et al., *NDT. E. Int.* **79** (2016) 109.
- [6] P. Caron et al., *Math. Sci. and Eng.* **61** (1983) 173.
- [7] M. Benyoucef et al., *Math. Sci. and Eng.* **234-236** (1997) 692.
- [8] M. Zietara et al., *Mater. Charact.* **87** (2014) 143.
- [9] A. Gaubert et al., *Acta Mater.* **84** (2015) 237.
- [10] M. Jouiad et al., *Mater. Sci. Forum* **706-709** (2012) 2400.
- [11] H. Mughrabi, *Mater. Sci. Tech.* **25** (2009) 191.
- [12] A. Gameros et al., *CIRP J. Manuf. Sci. Tec.* **9** (2015) 116.
- [13] B. Cai et al., *Acta. Mater.* **76** (2014) 371.
- [14] I.S. Anderson, R.L. McGreevy, H.Z. Bilheux, *Neutron Imaging and Applications: A Reference for the Imaging Community* (New York: Springer, 2009) 338 p. ISBN 978-0-387-78693-3.
- [15] E.H. Lehmann et al., *Int. J. Mater. Res.* **105** (2014) 664.
- [16] S. Peetermans et al., *J. App. Phys.* **114** (2013).
- [17] A.V. Rutkauskas et al., *J. Surf. Invest.: X-ray, Synchrotron, Neutron Tech.* **9** (2015) 317.
- [18] D.P. Kozlenko et al., *Phys. Part. Nuclei Lett.* **13** (2016) 346.
- [19] D.P. Kozlenko et al., *Phys. Procedia.* **69** (2015) 87.
- [20] C.A. Schneider et al., *Nat. Methods* **9** (2012) 671.
- [21] R.C. Chen et al., *J. Synchrotron Radiat.* **19** (2012) 836.
- [22] R.P. Dougherty et al., *Microsc. Microanal.* **13** (2007) 1678.
- [23] S.A. Hoseini et al., *Proceeding from the Third International Mechanical Engineering Conference, Tehran, Iran, (1998)* 947.
- [24] R.C. Reed et al., *Mater. Sci. Eng.* **448** (2007) 88.
- [25] X. Huang et al., *Pro. Nat. Sci. Mater.* **26** (2016) 197.